ANALYSIS OF A CONTINUOUS CURVED BOX GIRDER BRIDGE

C. Yoo,* Marquette University;
J. Buchanan, Ralph M. Parsons Company, Los Angeles;
C. P. Heins, University of Maryland; and
W. L. Armstrong, Federal Highway Administration

An analytical method for determining the response of horizontally curved bridges to loads is discussed. The predicted behavior of a curved box bridge under construction was compared to the actual behavior of such a bridge. The superstructure of the bridge tested consists of twin steel box girders in composite action with a 10-in. (25.4 cm) reinforced concrete slab. The portion of the bridge examined in this study was a three-span continuous structure designed for two-lane traffic. Two experimental testing programs were performed on the bridge. The first consisted of measuring the response of the steel box girders when a concrete deck was poured. When the construction of the bridge was completed, a second testing program involved measuring throughout the structure deformations and strains induced by the load of an FHWA test vehicle. Stresses, deformations, and load distributions are plotted, tabulated, and discussed. Comparisons of the analytical predictions, design values, and measured responses of the bridge are also presented.

•AS THE Interstate Highway System has grown, the demand for curved viaducts has increased. Curved viaducts are an efficient means of routing traffic at a multilevel interchange and thus optimize the use of limited rights-of-way. When curved alignments were introduced, they were generally composed of a series of straight girders used as chords, which dictated shorter spans, a large number of support units, large overhanging slabs, and less continuity.

Recently, however, sophisticated analytical methods for the design and analysis of curved girder bridges have been developed. One method of analysis (11, 12) was developed in 1973 at the University of Maryland. The analytical technique is based on differential equations that describe the behavior of single curved girders by using the finite difference and matrix displacement methods (10). The resulting equations are used to determine the response of nonprismatic single curved girders (CURSGL) and curved bridge systems (CURSYS) through use of computer programs (11, 12). Comparison of the results obtained from these analytical techniques (deflections, rotations, bending moments, vertical shears, St. Venant and warping torsion and bimoments) and those obtained from the experimental models (4, 9) shows excellent correlation.

This paper presents an analysis of a continuous curved box girder bridge and comparisons with the data based on the experiment conducted on the bridge. The correlation of analytical and experimental results establishes the effectiveness of and confidence in an analytical method for predicting the behavior of a curved box girder bridge. The bridge, instrumentation, test data, and formulation of an analytical model are described, and the results are discussed.

*When this paper was written, Mr. Yoo was visiting assistant professor, University of Maryland.

Figure 1. Plan of bridge.

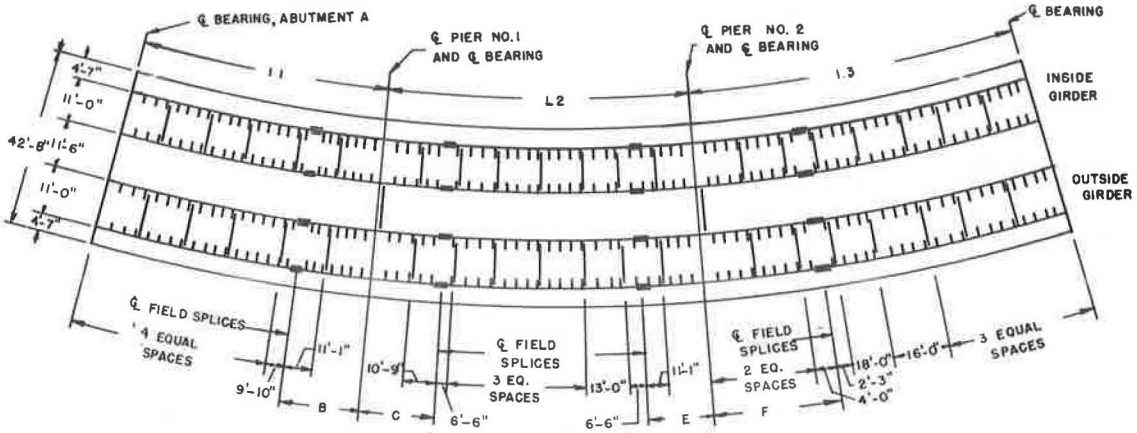

Figure 2. Typical cross section of bridge.

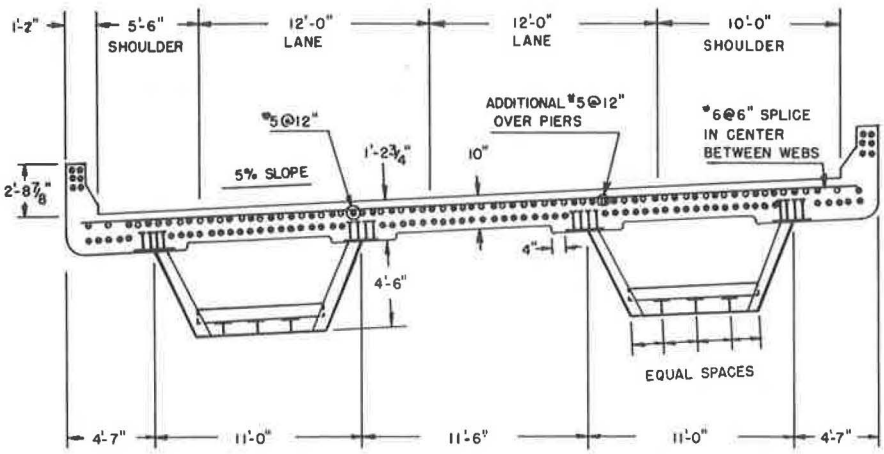

Figure 3. Detail of girder.

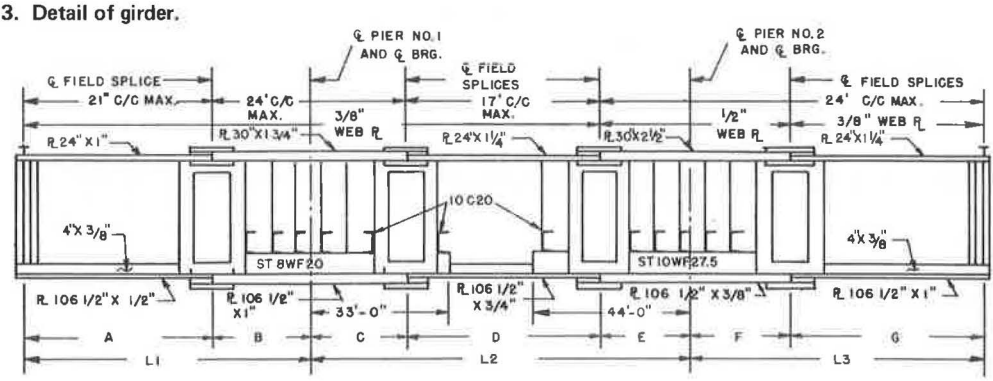

TABLE OF DIMENSIONS

GIRDER		A	B	L1	C	D	E	L2	F	G	L3	R
INSIDE	℄ LEFT TOP FLANGE	70'-6 3/4"	29'-2 15/16"	99'-9 11/16"	28'-0 5/16"	75'-2 3/8"	28'-0 5/16"	131'-3"	34'-7 5/16"	86'-1 7/8"	120'-9 3/16"	1300.981
	℄ RIGHT TOP FLANGE	71'-1 7/8"	29'-5 15/16"	100'-7 13/16"	28'-3 3/16"	75'-9 15/16"	28'-3 3/16"	132'-4 5/16"	34'-10 13/16"	86'-10 3/4"	121'-9 9/16"	1311.981
OUTSIDE	℄ LEFT TOP FLANGE	71'-9 3/8"	29'-9 1/16"	101'-6 7/16"	28'-6 3/16"	76'-5 13/16"	28'-6 3/16"	133'-6 3/16"	35'-2 1/2"	87'-7 15/16"	122'-10 7/16"	1323.481
	℄ RIGHT TOP FLANGE	72'-4 9/16"	30'-0"	102'-4 9/16"	28'-9"	77'-1 1/2"	28'-9"	134'-7 1/2"	35'-6"	88'-4 13/16"	123'-10 13/16"	1334.481

DESCRIPTION OF BRIDGE AND TESTING PROGRAMS

During fall 1973, the I-695 and I-83 interchange, C viaduct, located near Baltimore (Figure 1) was tested and analyzed for both dead and live loads. The superstructure consists of two large trapezoidal 4.5 by 11.0-ft (1.4 by 3.4-m) steel box girders with a 10-in. (25.4-cm) composite reinforced concrete deck (Figure 2). The bridge is a 12-span structure consisting of four units, each unit continuous over three spans. Unit 1 located at the north end of the bridge was selected for testing because it was most easily accessible in terms of elevation and existing traffic conditions. The bridge has a centerline radius of approximately 1,318 ft (402 m), and the span lengths are 100, 133, and 122 ft (30.5, 40.5, and 37.2 m) as shown in Figure 3.

The design of unit 1 is typical of that of the other three units. It was fabricated of five sections of steel, spliced at four locations of zero or small bending moment in the longitudinal direction as shown in Figures 1 and 3. The sections over the interior supports were designed under the assumption that the reinforced concrete deck does not yield composite action; however, the designer included shearing studs throughout the length. In the analytical model, it was assumed that the 10-in. (25.4-cm) concrete deck acted compositely. The dimensions for both boxes at any given point in the longitudinal direction are the same. The typical cross-sectional dimensions of unit 1 are shown in Figure 2. Details of construction can be found elsewhere (5).

Two testing programs were conducted on the bridge during two phases of construction. The first, the dead load test, measured the response of the bridge to the different phases of the placement of concrete deck. The second program, the live load test, measured the stresses and deformations induced by the load of an FHWA test vehicle on the completed structure.

Instrumentation

Eighteen rosette and 72 uniaxial strain gauges were mounted at four locations in the longitudinal directions (Figure 4). FHWA deflectometers were used. The response of the gauges was recorded on a 100-channel automatic digital strain indicator and two 10-channel portable units for dead load and on an FM analog tape recorder and oscillographs for live load.

Dead Load

The four locations of the strain gauges were selected on the basis of where the maximum positive and negative bending moments were expected to occur. The concrete was placed for each of the five steel sections separately by using the splice locations as boundaries. A summary of the dead load test results is given in Tables 1 and 2. The design values given in the tables were obtained directly from the designer. The design values shown for LL+I are not comparable with analytical and experimental values because the design loading condition was not consistent with the analytical and experimental loading condition.

Live Load

An FHWA test vehicle simulating an HS20-44 truck loading was used. The actual load distribution for the vehicle was 10,250 lb (4650 kg) on the front axle, 32,500 lb (14 750 kg) on the drive axle, and 31,750 lb (14 400 kg) on the trailer axle. The gross weight of the vehicle was 74,500 lb (33 800 kg).

The test was designed to measure the response of the bridge at various positions and speeds of the test vehicle. The vehicle traversed the bridge in four specified lanes (Figure 5) at speeds ranging from a crawl of 2 mph (3.2 km/h) to 50 mph (80 km/h).

Figure 4. Locations of (a) longitudinal and (b) transverse strain gauges.

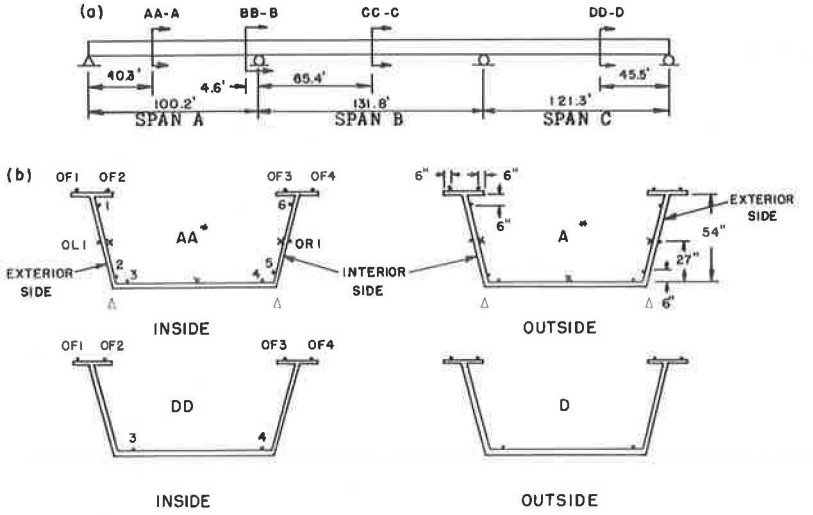

Δ Deflectometer Section AA-A (Section CC-Δ Exterior Sides only)

• UNIAXIAL GAGE

× ROSETTE GAGE

■ SAME GAGE LOCATION FOR SECTIONS BB-B AND CC-C, EXCEPT GAGES OL1 AND OR1 WHICH ARE PRESENT ONLY AT AA-A

Table 1. Comparison of experimental, analytical, and design deflections.

Location	Loading	Maximum Deflection (in.) Experimental	Analytical With Bracing[a]	Analytical Without Bracing[a]	Design	Allowable[b]
Δ 1-4	DL	1.19	0.88	0.93	1.00	
	LL+I	0.20	0.23	0.23	0.61	
	DL+LL+I	1.39	1.11	1.16	1.61	1.50
Δ 5, 6	DL	0.50	0.51	0.47	0.69	
	LL+I	0.26	0.27	0.27	0.94	
	DL+LL+I	0.76	0.78	0.74	1.63	1.98

Note: 1 in. = 2.5 cm.

[a]The impact factor applied to the analytical deflections for LL+I is based on the maximum average impact factor of 28.6 percent measured experimentally.

[b]According to AASHTO (span length/800).

Table 2. Comparison of experimental, analytical, and design stresses.

Section	Loading	Maximum Normal Stress at Bottom Flange (ksi) Experimental[a]	Analytical With Bracing	Analytical Without Bracing	Design	Allowable
A	DL	+7.70	+6.25	+9.02	+9.31	
	LL+I	+2.32	+2.65	+2.65	+6.86	
	DL+LL+I	+10.02	+8.90	+11.67	+16.17	+19.36
B	DL	-5.14	-4.96	-6.66	-11.51	
	LL+I	-0.76	-1.05	-1.05	-4.73	
	DL+LL+I	-5.90	-6.01	-7.71	-16.24	-19.63
C	DL	+6.12	+3.26	+4.27	+7.06	
	LL+I	+1.83	+2.07	+2.07	+6.97	
	DL+LL+I	+7.95	+5.33	+6.34	+14.03	+19.78

Note: 1 ksi = 6.9 MPa.

[a]Experimental dead load stresses were limited in quantity. Therefore, those shown may not be the maximum although they should be representative.

The crawl speed was assumed to eliminate virtually all dynamic effect of the moving vehicle.

Too few rosette gauges were mounted to justify a comparison of the measured shearing stresses with those obtained analytically. To reduce the test data, various computer programs were used (5). A summary of the results is shown in Figures 6 and 7 and in Table 2.

ANALYTICAL MODEL

Detailed descriptions of the two programs used in the analysis can be found elsewhere (12). Capabilities of these programs are given in Table 3. For the dead load test, the only structural member to connect the two boxes was the steel corrugated sheet, which was assumed to have negligible effects. Because there would be no interaction between the two boxes, each girder would act independently and the results from CURSGL would be identical to those from CURSYS. CURSGL was therefore selected for the dead load analysis, and CURSYS was used for live load analysis. Variations in the dimensions of the longitudinal cross section were incorporated by treating the governing differential equations with variable coefficients. To eliminate the numerical disturbance, it was assumed that the variation of the section properties spread to several nodal points in each side.

Dead Load Analysis

Top lateral bracing was added to the design to prevent excessive distortions of the cross section during the placement of concrete. This bracing in effect changed the configuration of the box girder from an open cell to a semiclosed cell. Therefore, both open cross section and closed cross section properties were used in the dead load analysis. To determine the section properties of the closed section, the top lateral bracing was replaced with an equivalent plate of constant thickness t_{eq}, determined from an equation developed by Dabrowski (6) and checked against equations developed by Kollbruner and Basler (8). The values from these two equations are approximately the same. The transverse K-bracing and the longitudinal lateral stiffeners were not included in the determination of section properties. The section properties were determined from a program developed by Blank (3). Properties used in the analytical procedure for sections with and without top bracing are given in Table 4.

The loading scheme in CURSGL requires vertical or torsional loads to be applied directly to the center of the girder. The total vertical load of concrete deck per unit length in the longitudinal direction, acting at the center of mass, was resolved into the centerline of the curved element with an equivalent vertical and torsional load. The bending stresses were computed by using

$$\sigma_f = M_x * c/I_x$$

The warping normal stresses were calculated by using

$$\sigma_w = BM * W_n/I_w$$

These stresses were then superimposed to obtain the final normal stresses, σ_t.

Figure 5. Location of lanes for test vehicle.

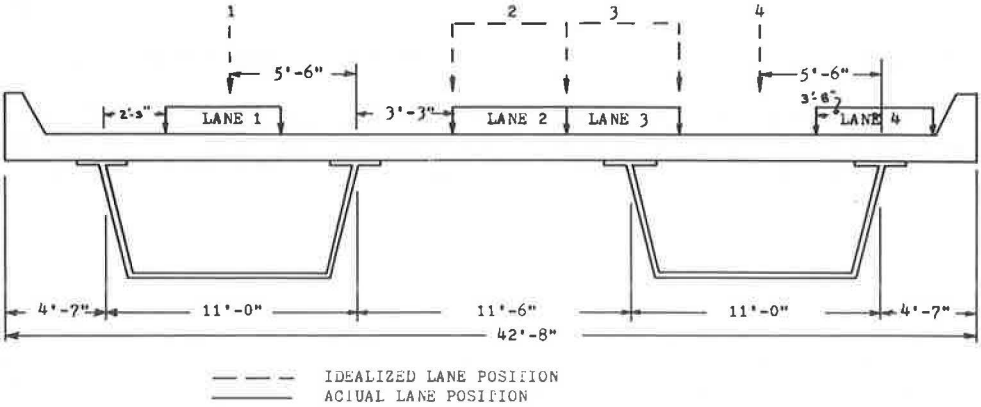

Figure 6. Normal stress, live load test (load point 3).

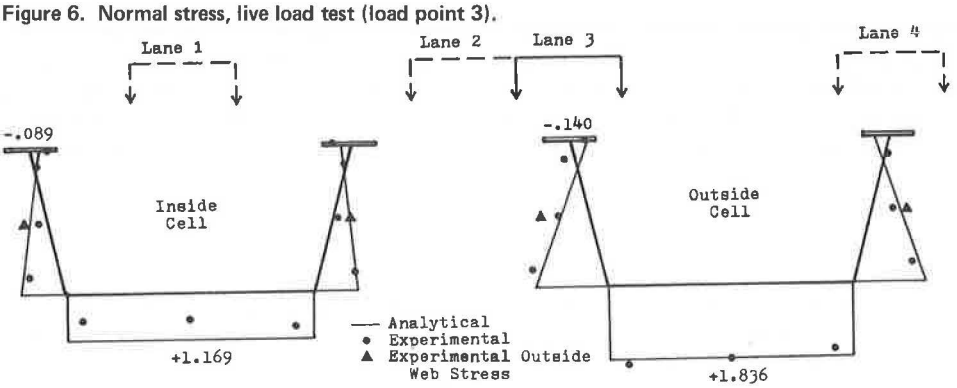

Figure 7. Normal deflection, live load test (load point 4).

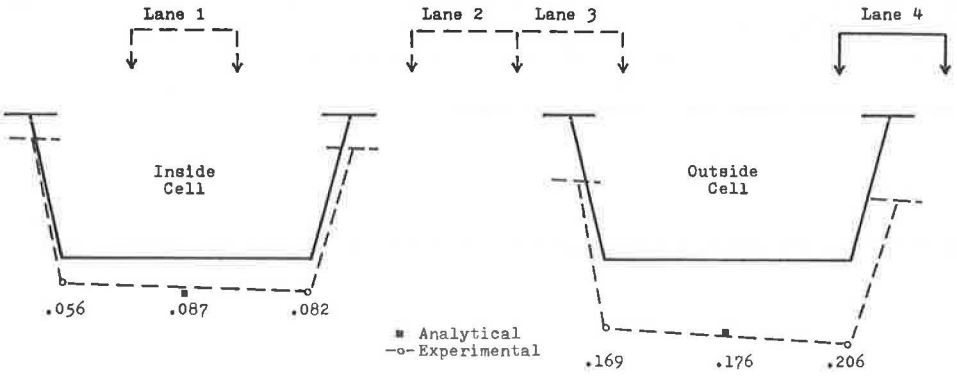

Table 3. Capabilities of CURSGL and CURSYS programs.

Capability	CURSGL	CURSYS
End support conditions may be either fixed or pinned or a combination in bending and torsion.	Yes	Yes
Simple span and multispan can be considered.	Yes	Yes
Dynamic storage allocation and segmentation are used.	No	Yes
Supports and diaphragms are assumed to lie along the radial direction, and diaphragms can be placed at any arbitrary locations and spacing.	—	Yes
Composite or noncomposite girder may be analyzed.	Yes	Yes
Girders are assumed to be equally spaced and concentric, and each girder is assumed to have a constant radius of curvature.	Yes	Yes
Cross-sectional properties may be varied from girder to girder and also along the span of each individual girder.	Yes	Yes
Any type of diaphragm (beam, truss, etc.) may be considered.	—	Yes
Any combination of dead and live loads may be considered for a given structure. Many loading cases may be considered for the given structure.	Yes	Yes
Deflections, rotations, bending moments, shear, bimoments, St. Venant torsion, warping torsion are evaluated at each nodal point.	Yes	Yes

Live Load Analysis

CURSYS was used in the live load analysis. The bridge model consisted of two curved elements with section properties equivalent to those of the box girders. The elements were connected with discrete diaphragms having equivalent transverse stiffness representing the concrete deck (12). These composite section properties were again computed by SECTP (3); the resulting values are given in Table 4.

The transverse stiffness of the concrete deck was idealized by specifying the discrete diaphragm between two girders at each nodal point. Average nodal spacing was 31.91 in. (81 cm). The concrete deck was transformed to an equivalent area of steel, as was done in the case of composite section. Reinforcing bars in the transverse direction were also added to the final stiffness properties.

Concentrated truck wheel loads were inputed into CURSYS in a manner that produced maximum stresses. The individual wheel loads were automatically resolved into concentrated vertical and torsional load with respect to each adjacent nodal point. The locations of the truck wheel loads are shown in Figure 8.

The stiffness coefficients for the discrete diaphragms are a function of flexural rigidity and effective length, L_t. Because CURSYS was written such that each girder is connected at the centerline, the effective length of the equivalent discrete diaphragm connecting each box varies considerably and is not readily determined. To determine the effective length of the equivalent diaphragm, we computed the normal stresses for one test vehicle position at five different effective lengths, which varied from 108 to 270 in. (274 to 685 cm). The 108-in. (274-cm) dimension represents the distance between two extreme inner flanges, and 270 in. (685 cm) is the distance between the centerlines of two girders. The analytical stress ratio was then determined for each of these lengths by forming a ratio of the analytical stress in the bottom flange of one box to the stress of the other box. The experimentally measured stresses for the bottom flange of each cell were averaged, and then the average stress was divided by the average stress of the other box to determine the experimental stress ratio. Comparison of each analytical stress ratio with the experimentally determined value indicated that the effective length can be taken as the average of the shortest distance of unsupported concrete length and the length between the centerlines of two adjacent box girders. For this bridge, the effective length of 189 in. (480 cm) had a ratio of stress distribution within 3 percent of that measured experimentally.

The normal warping stresses were computed and were on the order of 0.1 percent of the normal bending stresses, as expected. Therefore, the normal stresses for the live load analysis were entirely based on plane bending stresses. Thus, the neutral axis was assumed to lie parallel to the bottom flange, and the analytical stress distribution at any given height from the neutral axis on the cross section was constant.

DISCUSSION OF RESULTS

Dead Load

The normal stress distribution determined analytically is composed of the normal bending stress and normal warping stress. The normal bending stresses determined analytically account for approximately 95 percent of the total normal stresses in the section with lateral bracing. The experimental normal stresses are generally larger than those determined analytically. The low percentage of gauges in working order for the dead load test does not justify a conclusive statement on the normal stress distribution. However, those gauges that were functioning properly generally indicated a fair correlation with the analytically obtained normal stresses. A sample plot of normal stress distribution is shown in Figure 9. The experimentally measured deflections agreed well with those predicted by CURSGL for the first two pours of concrete, but the values for pour three did not agree so well. A similar trend was also noted by Greig (7). This may be attributed to the initial setting of the concrete. A sample deflection plot is shown in Figure 10.

Table 4. Section properties for dead load test.

Section	Analytical I_x (in.^{4})	Analytical I_w (in.^{6})	Analytical K_t (in.^{4})	Analytical A (in.^{2})	Analytical $\bar{y}$ (in.)	Design I_x (in.^{4})
No top bracing						
1	85872	124600000	22.39	143.00	26.00	85373.2
2	172310	249200000	144.6	253.25	26.84	171191.8
3	114260	160600000	48.18	181.62	24.05	90161.7
4	245520	347300000	409.5	352.10	27.27	244623.1
5	128730	182800000	68.71	208.25	20.97	120867.2
Noncomposite section, 0.042-in. bracing						
1	89664	84600000	57630	148.03	26.961	
2	175720	158200000	62900	258.01	27.341	
3	118650	105100000	59170	186.66	24.854	
4	248820	245800000	65560	356.86	27.630	
5	134120	117200000	59920	213.28	21.751	
Modified composite section[a], 2.64-in top flange						
1	212153	342500	344500	523.62	49.704	
2	374771	46780000	431700	648.89	46.047	
3	280686	15060000	395200	563.53	47.717	
4	496350	60540000	576300	765.71	44.230	
5	341320	4149000	424400	590.16	45.565	

Note: 1 in. = 2.5 cm; 1 in.^{2} = 6.45 cm^2; 1 in.^{4} = 41.6 cm^4; 1 in.^{6} = 26.8 cm^6.

[a]Live load test.

Figure 8. Analytical load point location for static live load test.

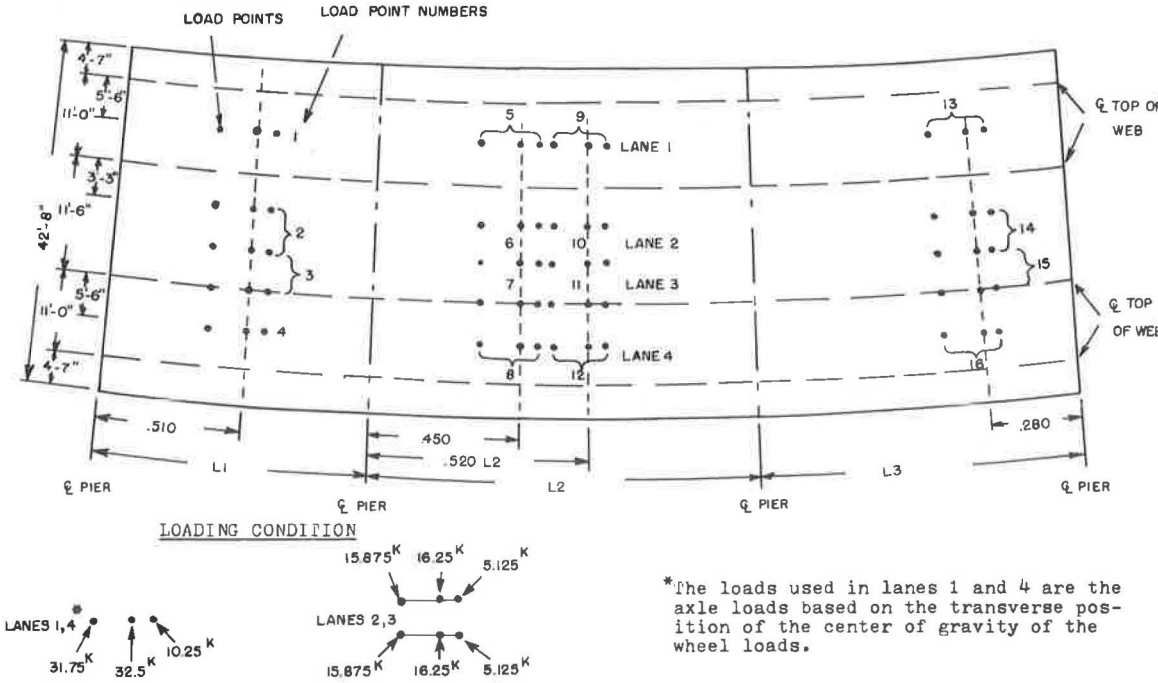

*The loads used in lanes 1 and 4 are the axle loads based on the transverse position of the center of gravity of the wheel loads.

Figure 9. Normal stress, dead load test (pour two).

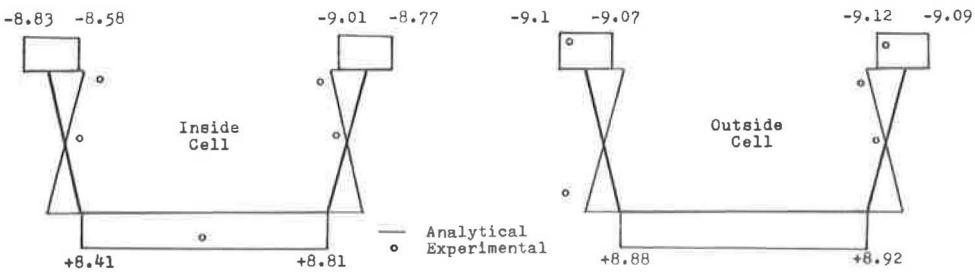

Figure 10. Normal stress, dead load test (pour three).

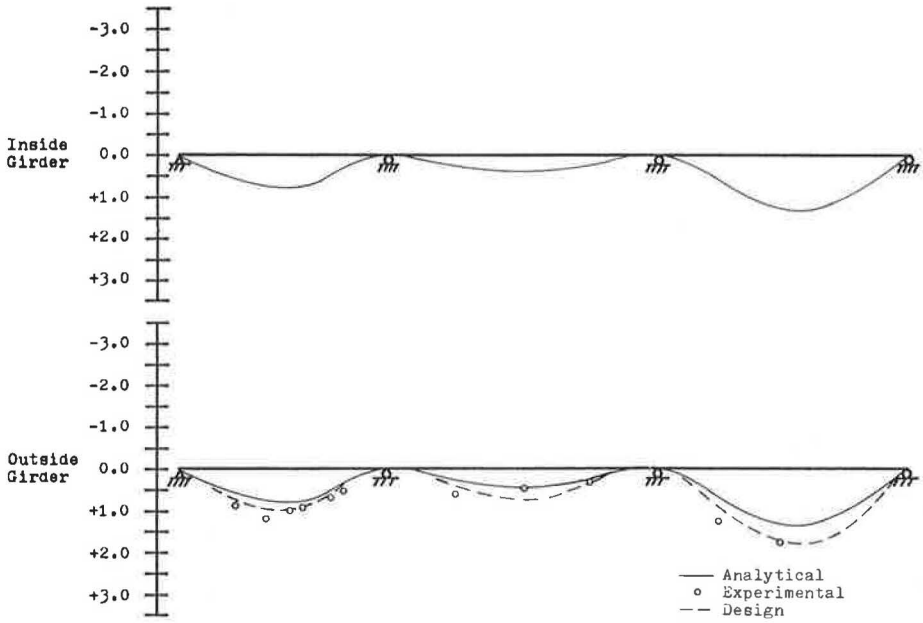

Live Load

The normal stresses obtained analytically generally agreed well with the measured stresses (Figure 6). However, the gauge at the top of the left web on the outside box deviated considerably from the analytical stress. This may be due to the local effect, i.e., the wheels of the test vehicle passing in the vicinity of the gauge. This local effect is most significant on the gauges at the top of the web. This phenomenon deserves further study.

Four strain gauges were mounted on the outside of the box at approximately upper midheight of the webs (section AA-A) so that possible web bending could be observed. Stresses measured on these gauges are shown in Figure 11. Note that the stresses on the outside of the web were consistently larger than the stresses on the inside, which indicates that the vertical webs of each cell bulged out. This trend is somewhat contradictory to that noted by Armstrong (2), which points to the need for further study in this area.

The analytical and experimental transverse load distribution factors were evaluated for each of the four sections where gauges were located. The distribution factor computed according to the AASHO specification (1) for two truck lane loadings on the bridge under study was 2.93. The truck positions are for those lanes that yield the most critical loading condition: lanes 3 and 4 in this study (Figure 5). The analytical and experimental distribution factors, therefore, were computed by adding the values from lanes 3 and 4 at each of four sections. The experimental distribution factors for the four sections ranged from 2.46 to 3.01 with an average value of 2.73. This accounts for 93 percent of the value given by AASHO. The analytical values ranged from 2.54 to 2.64 with an average of 2.58. The lower value for the analytical distribution factor would be expected because the designated lane position 4 was idealized closer to the center of the two girders than it was for the actual truck position in the field test.

The analytical and experimental deflections yield an excellent correlation as shown in Figure 7. The analytical and experimental rotations were also compared when the test vehicle was in lanes 1 through 4. The magnitude of the experimental rotations was generally within 15 percent of those predicted by analysis. The loading scheme for CURSYS was unable to place any loadings beyond the centerline of two outside

girders. CURSYS is being modified to eliminate this inconvenience. However, the idealization of the positioning to the test vehicle in lanes 1 and 4 had little effect on the normal stresses and deflections, but the effect on the rotations and corresponding torsional behavior was rather significant.

Impact

No dynamic analysis was made for comparative purposes. The experimentally measured values, however, were used to compute the impact factors. Averaging the 10 highest impact factors yielded a stress impact factor of 34.3 percent and a deflection impact factor of 31.4 percent. It should be noted that the live load stresses were small with a maximum of 2.15 ksi (14.8 MPa); thus, a conclusive statement may not be justified. The oscillograph trace exhibited somewhat steady-state frequency of vibration of 3 or 4 Hz.

FINDINGS AND CONCLUSIONS

The experimental normal stresses for the dead load test (Table 1) clearly show that the actual behavior of the box girders was somewhere in between the assumptions of open and closed cross sections as expected. The analyses were conducted by assuming the section properties with and without top transverse bracing. The torsional stiffness of the closed section was much higher (on the order of 200 or 1,000 times) than the open section stiffness, but the bending stiffness was essentially the same. This difference in torsional rigidity contributed to reduction in the warping normal stresses such that the total normal stresses account for approximately 30 percent for the open section to 5 percent for the closed section, even though the subtended angle of the bridge under study was relatively small. This suggests that the lateral bracing in the box section should be added inherently to prevent excessive distortions of the steel section when a concrete deck is poured.

The design of the box girders did not include any consideration of the lateral bracing or composite action over the supports, even though the design included standard shear studs throughout the length of the bridge. The design stresses are much higher than those determined analytically, with consideration of top bracing (Table 2).

Generally, the experimental results were predicted well by the analysis. Correlation of the analytical and experimental results for the live load tests yielded a maximum deviation of 10 percent, which indicates that the analytical method is accurate and effective. However, as can be seen in Figure 6, the normal stresses at the middle of the bottom flange were always smaller than the ones under the web because of shear lag. Currently, CURSYS only gives the average stresses.

It is interesting to note the close correlation between the distribution factors determined experimentally and the AASHO value, indicating that the equation given in the AASHO specifications is valid. AASHO recommends that a simple beam isolation be made for a large girder spacing for steel I-beam, concrete T-beam, timber stringer, and concrete box girders. The results obtained in this study clearly show that a simple beam idealization would be very conservative inasmuch as the distribution factor thus obtained would be 3.51.

ACKNOWLEDGMENTS

This research was conducted as a cooperative project of the Civil Engineering Department, University of Maryland; the Maryland Highway Administration; and the Federal Highway Administration. Their encouragement and guidance are gratefully acknowledged.

REFERENCES

1. Standard Specifications for Highway Bridges, 10th Ed. American Association of State Highway Officials, 1969.
2. W. L. Armstrong and J. A. Langdon. Dynamic Testing of a Curved Box Beam Bridge. Federal Highway Research and Development Report 73-1, Feb. 1973.
3. D. Blank. Stiffening of Box Beam Using Corrugated Shapes. Department of Civil Engineering, Univ. of Maryland, MS thesis, Aug. 1973.
4. B. Bonakdarpour, L. C. Bell, and C. P. Heins. Analytical and Experimental Study of a Curved Bridge Model. Univ. of Maryland, Civil Engineering Rept. 36, June 1970.
5. J. Buchanan. Experimental and Analytical Study of a Curved Box Girder Bridge. Department of Civil Engineering, Univ. of Maryland, MS thesis, June 1974.
6. R. Dabrowski. Curved Thin-Walled Girder Theory and Analysis. Cement and Concrete Association, England, Translation 144, 1968.
7. R. A. Greig. Field Testing of a Curved Steel Box Girder Bridge in Springfield, Massachusetts. Univ. of Rhode Island, Technical Rept. 1 (L), March 1973.
8. C. F. Kollbrunner and K. Basler. Torsion in Structures. Springer-Verlag, 1969.
9. K. R. Spates and C. P. Heins. The Analysis of Simple Curved Girders With Various Loadings and Boundary Conditions. Univ. of Maryland, Civil Engineering Rept. 20, June 1968.
10. V. Z. Vlasov. Thin-Walled Elastic Beams. National Science Foundation, 1961.
11. C. Yoo, D. Evick, and C. P. Heins. Non-Prismatic Curved Girder Analysis. Journal of Computers and Structures, London, Vol. 3, 1973.
12. C. Yoo and C. P. Heins. Users Mannual for the Static Analysis of Curved Bridge Girders. Univ. of Maryland, Civil Engineering Rept. 55.